THE CONTENT OF HYDROGEN TO THE EFFECT ON THE COMBUSTION CHARACTERISTICS OF BIOMASS-DERIVED SYNGAS

by

Guoyan CHEN[a], Zheng SHEN[a], Junsheng ZHANG[b*], Shuangshuang ZUO[a], Anchao ZHANG[a], Haoxin DENG[a], Yanyang MEI[a], and Fanmao MENG[a]

[a]School of Mechanical and Power Engineering, Henan Polytechnic University, Jiaozuo, China
[b]Institute of Resources and Environment, Henan Polytechnic University, Jiaozuo, China

Original scientific paper
https://doi.org/10.2298/TSCI220418113C

Biomass-derived syngas is prone to leakage during transportation. To safely use biomass-derived syngas, we need to study the combustion characteristics of material syngas the purpose of this paper is: at T = 303 K, P = 0.1 MPa, under the condition of the spherical expansion flame method, calculate the laminar burning velocity, and used the Chemkin module of ANSYS to simulate four mechanisms (GRI-3.0, FFCM-1, Li-2015, SanDiego +NO_x-2018) to compare, select more appropriate reaction mechanism through experimental data for related research. It was found that the chemical reaction mechanism of GRI-3.0 is more in line with the experimental results. It is found that the experimental results are in good agreement with the linear extrapolation method. When the H_2 concentration increases from 22-42%, the peak laminar burning velocity moves in the direction of the lean fuel side. When the H_2 concentration increases to 42%, the laminar burning velocity is the fastest, reaching 0.78 m/s. The effect of H_2 on thermal diffusivity is high. When H_2 concentration reaches 42%, its thermal diffusivity is much higher than other gas components. The adiabatic flame temperature of F1 (22% H_2, 45% CO, 9.6% CH_4, 23.4% CO_2)-air mixtures is the highest, approaching 2196 K. The peak adiabatic flame temperature of F5 (42% H_2, 25% CO, 9.6% CH_4, 23.4% CO_2)-air mixtures is 2082 K, which is comparatively low. Nonetheless, the H_2 concentration in F5-air mixtures is higher than that in F1-air mixtures, indicating that H_2 has less influence on adiabatic flame temperature than CO. The positive reactions to accelerate laminar burning velocity mainly include R99, R38, and R46. The R52 and R35 can inhibit laminar burning velocity. There are many factors affecting laminar burning velocity, among which high reactive free radicals are the main factors, and the competition between chain branching reaction and chain termination reaction for high reactive free radicals also affects laminar burning velocity. With the increase of concentration of H_2, participate in the reaction of the molar mass fraction of highly reactive free radicals and the laminar burning velocity.

Key words*: safety engineering, biomass-derived syngas, H_2 effect, laminar burning velocity*

*Corresponding author, e-mail: 10460200494@hpu.edu.cn

Introduction

Technology of biomass-derived syngas, low quality biomass energy can be converted into combustible gas with high calorific value, it has high potential in future energy development, reduced consumption of fossil fuels [1]. But, in the transportation process, the biomass-derived syngas often leakage [2, 3], because it contains more CO, H_2, CH_4, and other flammable gases, it is liable to explode when exposed to the open flame and becoming very dangerous [4, 5].Therefore, the burning characteristics of biomass-derived syngas are of great significance.

At present, many experts at home and abroad have done a lot of research on biomass energy. The laminar burning velocity of biomass-derived syngas (20%H_2, 20%CO, 60%N_2) under low pressure was measured by the Angle method by Ma *et al*. [6] and Liu *et al*. [7]. In the 1951 years, the existence of special cellular flame structures in premixed flames by Garside and Jackson *et al*., lays a foundation for studying the influence of thermal diffusion instability on laminar flame. The external heating divergent channel method is used by Varghese *et al*. that the laminar burning velocity of H_2/CO/CH_4/CO_2/N_2-air flame at high temperature was experimentally measured, two linear models for predicting the laminar burning velocity of variable component syngas mixtures are presented. Law and Kwon [8], the method of spherical flame expansion is adopted that the laminar burning velocity of CH_4/H_2 mixture was measured and Markstein length and the process of cellular flame change, it is found that the laminar burning velocity of biomass-derived syngas decreases gradually with the addition of CH_4. The laminar burning velocity of CH_4/H_2-air mixtures in standard environment was measured by experiments by Huang *et al*. [9]. The effect of H_2 addition on flame spread of CH_4-air mixtures was studied by ways of digital analysis in combination with model tests by Wang *et al*., [10]. Ma *et al*. [11] studied that under standard conditions, the peak pressure arrived earlier than the peak temperature in the combustion process of CH_4/H_2-air mixtures, and the explosion pressure and temperature of the combustion chamber increased significantly with the addition of H_2. Momeni *et al*. [12] found the influence of catalyst type on H_2 content in biomass syngas is studied, which provides a theoretical basis for improving H_2 productivity. The addition of DME to low concentration methane gas shows that DME can promote the combustion of low concentration methane gas, which increases with the increase of pressure by William *et al*. [13]. The addition of HC significantly affects the flame rate of syngas mixtures by Keesee *et al*. [14]. Krejci *et al*. [15] studied the ignition delay time was investigated by kinetic modeling of H_2 and syngas fuel mixtures. It was found that the increase of CO content would prolong the ignition delay time.

On the basis of the study, the laminar flame combustion characteristics of material syngas were studied by changing the concentration of H_2 in different components of the biomass-derived syngas at T = 303 K, P = 0.1 MPa. The effect of H_2 concentration on the biomass-derived syngas was studied by gas reaction kinetics and sensitivity analysis.

Experiments and data processing

Experimental methods

The experiments in the current work were performed in a stainless steel constant-volume cylindrical combustion chamber to the laminar burning velocity of CH_4, H_2, CO, and CO_2 mixtures under different conditions were measured, fig. 1. Schematic of the experimental set-up. The test system comprises the high-speed camera system (Phantom Miro M 310) and the maximum resolution is 1024 × 1024 resolution. The high-speed camera connects

to the laptop and records the flame structure through the built-in camera control system. The constant volume combustion chamber, the ignition system, the gas control system, the data collection system, the pressure transducer. The constant volume combustion chamber has a steel cylinder with a volume of 6.3 L and inner diameter is 200 mm. The front and rear ends of the combustion chamber are equipped with two toughened transparent glass with a diameter of 170 mm and a thickness of 50 mm, as an optical observation window for the combustion chamber. The ignition system consists of a pair of tungsten wires with a diameter of 0.45 mm and spark plugs, link to ignition control switch via wire. In this experiment, we use JDYBS-C2 precision digital pressure sensor meter and MD-HF pressure sensor. The pressure is collected and analyzed by LabVIEW data acquisition system [16], using the high-speed camera control system, film the flame at 3200 fps. Used such a camera without a schlieren system to directly acquire flame images in the present work is not only more convenient and effective but also beneficial for observing the original shape of the flame. When the experiment, the initial temperature is set at 303±3 K, the initial internal pressure is controlled at 0.1 MPa, the equivalent ratio is set at 0.6-1.5, different proportions of CH_4, H_2, CO, and CO_2 were mixed, tab. 1, to simulate the biomass-derived syngas.

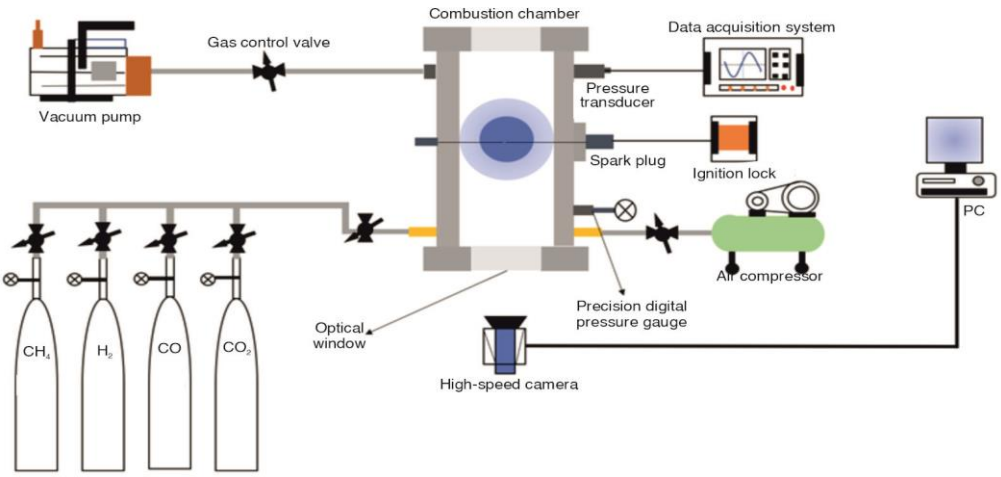

Figure 1. Schematic of the experimental set-up

Table 1. Fuel composition

	Fuel composition [vol.%]				Density [g/L]
	XH_2	XCO	XCH_4	XCO_2	
F1	22	45	9.6	23.4	0.938
F2	27	40	9.6	23.4	0.895
F3	32	35	9.6	23.4	0.851
F4	37	30	9.6	23.4	0.807
F5	42	25	9.6	23.4	0.763

First, we should make the combustion chamber be vacuumizing and fill the combustion chamber with different kinds of gases according to the simulated ratio of the biomass-derived syngas in tab. 1. At the end of charging, stand for 10 minutes. After the internal gas is fully mixed, the ignition device is used to ignite. The high-speed camera shoots syn-

chronously to record changes in the flame structure. After a group of experiments, the air compressor is used to exhaust the gas after the combustion. It is important that attention should be paid to the ventilation of the laboratory [17, 18]. In the exhaust process, the air can bring out the water generated by the experiment, so as to prevent water mist on the surface of the glass observation window from affecting the experiment. Finally, each set of experiments must be run several times to check stability.

Calculation of the laminar burning velocity

A spherical flame propagating outwards, its tensile flame velocity, S_b [19, 20]:

$$S_b = \frac{\mathrm{d}r_f}{\mathrm{d}t} \tag{1}$$

where r_f is the instantaneous spherical flame radius and the t – the time. The spherical flame stretching rate can be obtained from the following formula [21, 22]:

$$K = \frac{2S_b}{r_f} \tag{2}$$

where A is the area of the spherical flame, and the unstretched flame velocity S_b^0 is obtained in the formula [23, 24]:

$$S_b = S_b^0 - L_b K \tag{3}$$

where the L_b is the length of the Markstein. We can obtain the speed S_b^0 and the length L_b of the unstretched flame through the non-linear relationship between the speed of the stretched flame and the tensile rate of the flame. Its expression is [25, 26]:

$$\begin{aligned} K &= M\left(S_b\right)^2 - N\ln\left(S_b\right)^2 \\ M &= \frac{\ln\left(S_b^0\right)}{L_b S_b^0}, \quad N = \frac{1}{2L_b S_b^0} \end{aligned} \tag{4}$$

The laminar burning velocity, S_L, can be determined by a simplified continuity equation for the flame front [27, 28]:

$$\rho_u S_L = \rho_b S_b^0 \tag{5}$$

where ρ_u [kgm^{-3}] is the density of the burned gas and the ρ_b [kgm^{-3}] – the density of the unburned gas.

Numerical modeling

It is very convenient to use a high-speed camera to shoot the flame propagation image, which can clearly observe the original shape of the flame. Figure 2 shows the evolution process of flame under different equivalent ratios. It can be intuitively seen that with the change of the equivalent ratio, the flame propagates faster and faster, and the cell structure of the flame appears earlier. In this experiment, the Chemkin module under ANSYS software was used to simulate laminar flame combustion, tab. 2 the detailed mechanisms considered in this work. Figure 3 shows the simulation results of the four mechanisms. Compared with the experimental data of the F2 (27% H_2, 40% CO, 9.6% CH_4, 23.4% CO_2)-air mixtures, it was found that the gas of the F2-air mixtures is more consistent with the GRI-3.0 mechanism in this experiment. Different data processing methods also affect the flame stretching rate of

syngas. Figure 4 analyzes the experimental data of the F2-air mixtures with different equivalent ratios by means of linear and non-linear fitting. It is found that there is a gap between the two extrapolation methods, and linear is more suitable for the data of this experiment. After several experiments, the GRI-3.0 mechanism is more accurate after comparing laminar flame velocity of all gas components in fig. 5 with the simulation results of GRI-3.0 mechanism, and the error of the laminar burning velocity is 1-2 cm/s. The GRI-3.0 mechanism has been validated by extensive experimental results, including 53 components and 325 primitive reactions. The mechanism file includes three parts: chemical reaction mechanism, thermodynamics file and transport file. In simulation, the adaptive grid parameters of gradient and curvature are controlled within 0.02. In this study, the flame boundary was detected by Image-Pro Plus (IPP) software and the flame radius, r_f, was then determined.

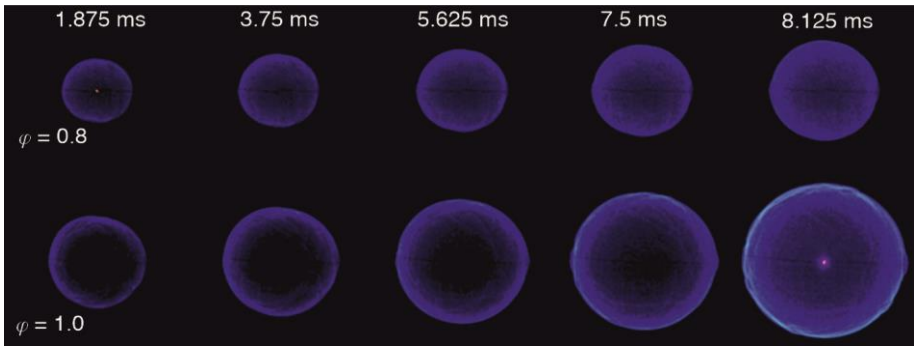

Figure 2. Flame propagation image with F2-air mixtures equivalent ratio of 0.8 and equivalent ratio of 1.0

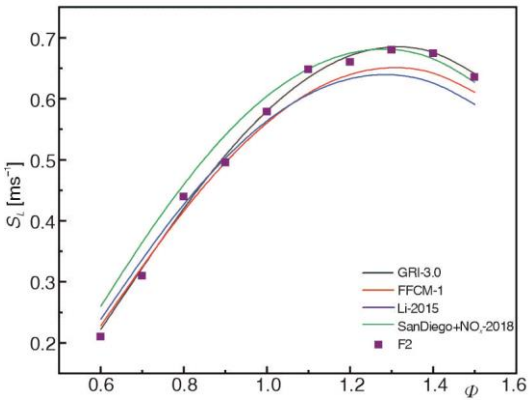

Figure 3. The F2-air mixtures experiments with four mechanisms to simulate the laminar burning velocity
(*for color image see journal web site*)

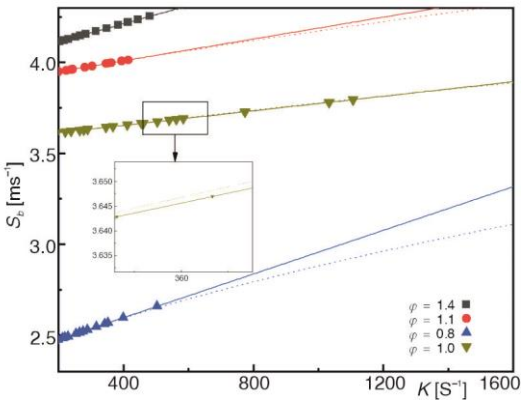

Figure 4. Stretch flame speed *vs.* stretch rate; solid line represents the linear method and dashed line represents the non-linear method

Table 2. The detailed mechanisms considered in this work

	Mechanism	Ref.
1	GRI-3.0	[29]
2	FFCM-1	[30]
3	Li-2015	[31]
4	SanDiego +NO_x-2018	[32]

Experimental analysis

The laminar burning velocity and thermal diffusivity and adiabatic flame temperature

Then T = 303 K and P = 0.1 MPa, it can be seen from fig. 5 that the laminar burning velocity reaches the maximum value when the equivalent ratio is 1.1-1.3. When the H_2 concentration is less than the CO concentration, the laminar burning velocity is low. When H_2 concentration increases from 22% to 42% and CO concentration decreases from 45% to 25%, the peak of the laminar burning velocity increases gradually. The relationship between the laminar burning velocity and pressure and temperature can be fitted by using:

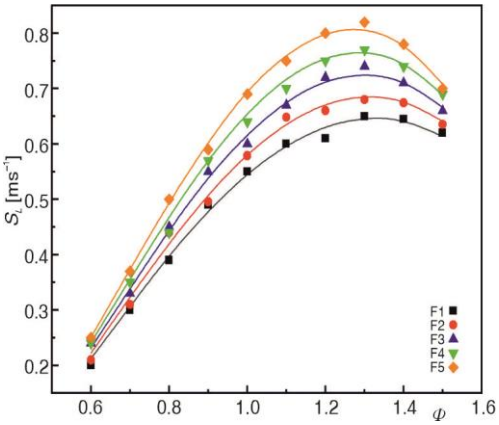

Figure 5. The laminar burning velocity that F1-F5-air mixtures experiment and simulation; solid line represents the model predictions and the symbols represent the experimental measurements

$$S_L = S_u(\Phi)\left(\frac{P_u}{P_0}\right) f(\Phi) \tag{6}$$

where $S_u(\Phi)$ [ms^{-1}] is the simulation laminar burning velocity, P0 – the initial pressure, and $f(\Phi)$– the pressure factor. In this experiment, P_u = P_0 = 0.1 MPa by fitting the experimental value of the F2-air mixtures, it can be obtained as:

$$S_L = -0.04427 + 0.8203\Phi - 0.17638\Phi^2 + 0.173\Phi^3 - 0.185424\Phi^4 \tag{7}$$

Figures 6 and 7 show the thermal diffusivity and adiabatic flame variation of each component gas. The laminar burning velocity is proportional to thermal diffusivity and adiabatic laminar temperature. With the increase of H_2 concentration, the equivalent ratio becomes larger, and the thermal diffusivity increases accordingly, making the peak of laminar flame velocity move to the right. The thermal diffusivity of gas components with a higher H_2 concentration is relatively high, while that of gas with a higher CO concentration is relatively low. In the simulation experiment, the adiabatic flame temperature decreases with increasing H_2 concentration, the adiabatic flame temperature of the F1-air mixtures with less H_2 content and more CO content is the highest among the five groups of gases. In contrast to the laminar burning velocity results, the laminar burning velocity manifests as the higher the H_2 concentration, the higher the velocity. Compared with CO, H_2 has relatively little influence on the adiabatic flame temperature of biomass syngas. Different data processing methods also affect the flame stretching rate of syngas. Figure 7 analyzes the experimental data of the F2-air mixtures with different equivalent ratios by linear and nonlinear fitting methods, and finds that there is a gap between the two extrapolation methods, and the linearity is more suitable for the data of this experiment.

Sensitivity analysis

Figure 8 shows the sensitivity analysis of F1 and F3 (32% H_2, 35% CO, 9.6% CH_4, 23.4% CO_2) and F5-air mixtures that equivalent ratio 1.3. The sensitivity coefficients were calculated using premixed codes in Chemkin to find out the basic reactions that affect the laminar burning velocity, a major positive dominant reaction: OH+CO→H+CO_2(R99), O_2+H→O+OH(R38), H+HO_2→2OH(R46), reactions that play a reverse-dominant role: H+CH_3(+M)→CH_4(+M) (R52), H+O_2+H_2O→HO_2+H_2O(R35).

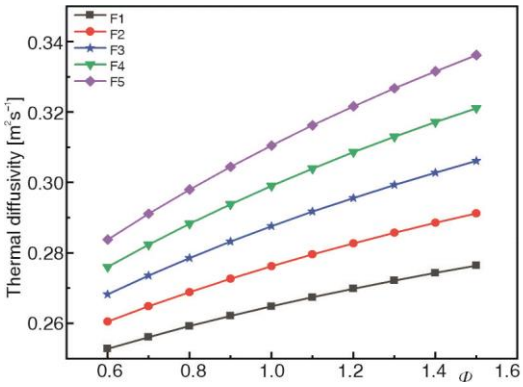

Figure 6. Thermal diffusivity of F1-F5-air mixtures

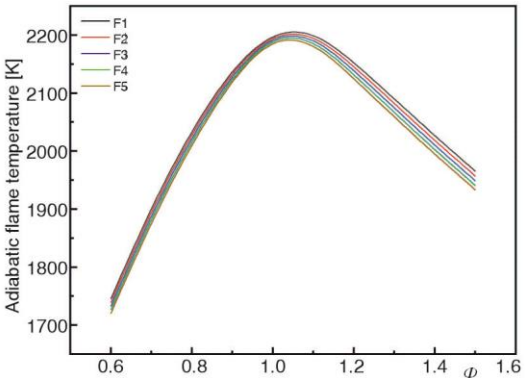

Figure 7. Adiabatic flame temperature of F1-F5-air mixtures
(*for color image see journal web site*)

In the forward dominant reaction, the main role is R99, R38, R46, R3; among them, R99 is an oxidation reaction, which generates a stable product CO_2 by consuming a large number of OH groups, and at the same time generates a large number of H groups during the reaction. The R38 and R3 are important chain branching reactions in this process. The former consumes H radicals to generate O radicals and OH radicals, while the latter consumes H_2 in the reaction to generate a large number of H radicals and OH radicals. The R46 generates OH radicals by consuming H radicals. The aforementioned positive and dominant reactions swiftly consume H_2 and CO in the reactants and generate a large number of highly reactive free radicals, thereby increasing the laminar combustion rate.

In the reverse dominant reaction, R35, R45, R53, and R87 play a major role. R45 and R53 consume the H radicals generated in the forward reaction, and the products O_2 and H_2 are the important reactants and products of the whole reaction. The R33 consumes O_2 to generate HO_2 to promote the reaction of R45. The R53 consumes H radicals and reacts CH_4 to generate H_2, which assists R3 to generate O radicals and OH radicals.

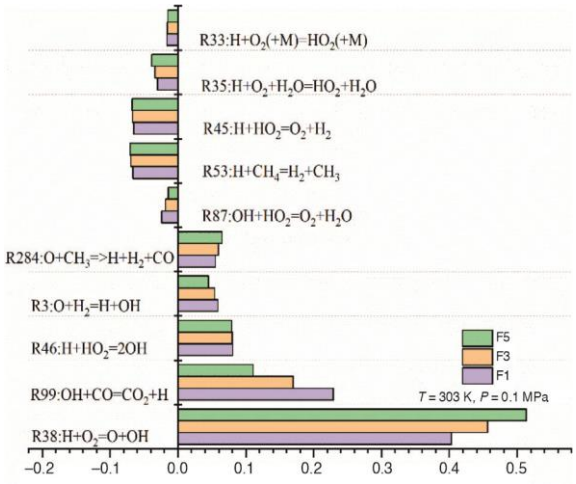

Figure 8. The sensitivity analysis of F1, F3, and F5-air mixtures that equivalent ratio 1.3

It can be seen from fig. 8 that with the continuous increase of H_2 concentration, the forward reaction is dominated by R99 to R38, absorbing a large amount of H radicals and O_2, and promoting the generation of OH radicals. The reverse reaction R35 consumes H radicals to attain a stable product H_2O to terminate the chain reaction, and R33 is also a chain termination reaction that consumes H radicals. These two reactions inhibit the acceleration of laminar combustion. Nevertheless, with the increase of H_2 concentration, at the same temperature and pressure, although the reverse reaction consumes H radicals, the amount produced by the forward reaction is many times the consumption. Therefore, due to

the continuous generation of highly active radicals O, OH, and H, the laminar burning velocity is promoted.

The effect of molar mass fraction

Figure 9 shows the change in the molar mass fraction of highly reactive radicals with different concentrations of H_2 when T = 303 K, P = 0.1 MPa, and the equivalence ratio is 1.3. In the sensitivity analysis of 3.2, the factors affecting the laminar burning velocity depend on the concentration of various active radicals. It can be seen from the figure that the order of magnitude of the mass fraction of highly active radicals (O, OH, H) is mainly distributed 1.1-1.4 near. The kinetic mechanism of the chemical reaction is composed of chemical reaction chain branching, chemical reaction chain transfer and chemical reaction chain termination. In the elementary reaction, highly reactive free radicals directly participate in the reaction and gradually convert the fuel into the final product. From fig. 9, it can be seen that in the syngas with different H_2 concentrations, the most content in the flame is H radicals, followed by OH radicals and O radicals. With the increase of H_2 concentration, the content of H radicals decreased slightly, which was due to the gradual replacement of OH+CO→H+CO_2 (R99) by the reaction O_2+H→O+OH(R38), while the H_2 concentration increased from 22% to 42%, the reaction rate of R38 decreases and the reaction of R99 increases, which is the main reason for the decrease of the molar mass fraction of H radicals in the fig. 9.

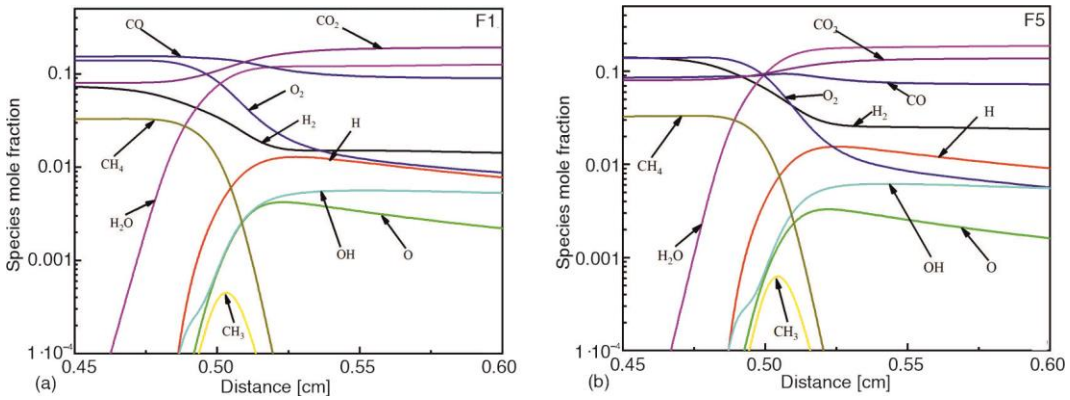

Figure 9. The species mole fraction of (a) F1 and (b) F5 air mixtures at T = 303 K, P = 0.1 MPa

Conclusions

In this experiment, under the conditions of initial temperature T = 303 K and initial pressure P = 0.1 MPa, the laminar combustion characteristics of five groups of syngas with different H_2 concentrations at equivalence ratios of 0.6-1.5 were analyzed. Through analysis and comparison of the data measured in the experiment, it was found that the chemical reaction mechanism of GRI-3.0 is more in line with the experimental results. The following are the main conclusions drawn from the experiment:

- After combining the experimental data of laminar flame with the simulation, it can be seen that the experimental results are in good agreement with the linear extrapolation method. When the H_2 concentration increases from 22% to 42%, the peak value of the laminar burning velocity increases with the equivalence ratio. When the H_2 concentration is 42% the laminar burning velocity is the fastest, reaching 0.78 m/s, H_2 has a high influence on thermal diffusivity. When the concentration of H_2 reaches 42%, its thermal diffusivity is much

higher than that of other gas components; the adiabatic flame temperature is opposite to the previous two. The adiabatic temperature of the F1-air mixtures with the CO concentration of 45% is the highest of all components, which is close to 2196 K, while the F5-air mixtures with the highest H_2 concentration has a peak adiabatic flame temperature of 2082 K, which is relatively low, indicating that the effect of H_2 on the adiabatic flame temperature is not as high as that of the CO.

- Through sensitivity analysis, it is found that the main forward reactions that accelerate the laminar burning velocity are: R99, R38, R46, while the reverse reactions that inhibit the laminar burning velocity are mainly: R52, R35; factors affecting the laminar burning velocity. There are many, highly reactive free radicals are the main factors, in which the competition between the chain branching reaction and the chain termination reaction for highly reactive free radicals also affects the laminar burning velocity. As the H2 concentration increases, the molar mass fraction of highly reactive radicals participating in the reaction increases, resulting in an increase in the laminar burning velocity.

Acknowledgment

The authors appreciate the support of the Innovative Research Team of Henan Polytechnic University (T2020-3) and the National Natural Science Foundation of China (Nos.51774115).

References

[1] Watanabe, H., *et al*., NOx Formation and Reduction Mechanisms in Staged O_2/CO_2 Combustion, *Combustion and flame, 158* (2011), 7, pp. 1255-1263
[2] Xiang, L., *et al*., Numerical Study on CH_4 Laminar Premixed Flames for Combustion Characteristics in the Oxidant Atmospheres of $N_2/CO_2/H_2O$/Ar-O_2, *Journal of the Energy Institute*, *93* (2020), 4, pp. 1278-1287
[3] Zhou, Q., *et al*., Effects of Fuel Composition and Initial Pressure on Laminar Flame Speed of H_2/CO/CH_4 Bio-Syngas, *Fuel, 238* (2019), Feb., pp. 149-158
[4] Yao, Z., *et al*., Experimental Study on Explosion Characteristics of Premixed Syngas/Air Mixture with Different Ignition Positions and Opening Ratios, *Fuel, 279* (2020), 118426
[5] Yao, Z., *et al*., On Explosion Characteristics of Premixed Syngas/Air Mixtures with Different Hydrogen Volume Fractions and Ignition Positions, *Fuel, 288* (2021), 119619
[6] Ma, A.-L., *et al*., Study on the Combustion Characteristics of the Bio-Briquette, *Journal of Henan Polytechnic University* (Natural Science), 2009
[7] Liu, Q., *et al*., Co-Firing of Coal and Biomass in Oxy-Fuel Fluidized Bed for CO_2 Capture: A Review of Recent Advances, *Chinese Journal of Chemical Engineering, 27* (2019), 10, pp. 2261-2272
[8] Law, C. K., Kwon, O., Effects of Hydrocarbon Substitution on Atmospheric Hydrogen–Air Flame Propagation, *International Journal of Hydrogen Energy, 29* (2004), 8, pp. 867-879
[9] Huang, Z., *et al.*, Measurements of Laminar Burning Velocities for Natural Gas–Hydrogen–Air Mixtures, *Combustion and Flame, 146* (2006), 1-2, pp. 302-311
[10] Wang, J., *et al*., Effect of Hydrogen Addition on Early Flame Growth of Lean Burn Natural Gas–Air Mixtures, *International Journal of Hydrogen Energy, 35* (2010), 13, pp. 7246-7252
[11] Ma, Q., *et al*., Effects of Hydrogen on Combustion Characteristics of Methane in Air, *International Journal of Hydrogen Energy, 39* (2014), 21, pp. 11291-11298
[12] Momeni, M., *et al*., Experimental Study on Effects of Particle Shape and Operating Conditions on Combustion Characteristics of Single Biomass Particles, *Energy & Fuels, 27* (2013), 1, pp. 507-514
[13] William, F.A., Diffusion Flames and Droplet Burning, in: *Combustion Theory*, CRC Press, Boka Raton, Fla., USA, 2018, pp. 38-91
[14] Keesee, C. L., *et al*., Laminar Flame Speed Measurements of Synthetic Gas Blends with Hydrocarbon Impurities, *Proceedings*, Turbine Technical Conference and Exposition, Montreal, Canada, 2015
[15] Krejci, M. C., *et al*., Laminar Flame Speed and Ignition Delay Time Data for the Kinetic Modeling of Hydrogen and Syngas Fuel Blends, *Journal of Engineering for Gas Turbines and Power, 135* (2013), 2

[16] Zhang, Q., *et al*., Experimental and Numerical Study of the Effects of Oxygen-Enriched Air on the Laminar Burning Characteristics of Biomass-Derived Syngas, *Fuel, 285* (2021), 119183
[17] Markstein, G. H., *Nonsteady Flame Propagation: AGARDograph*. Elsevier, Amsterdam, The Netherlands, 2014
[18] Halter, F., *et al*., Nonlinear Effects of Stretch on the Flame Front Propagation, *Combustion and Flame, 157* (2010), 10, pp. 1825-1832
[19] Ronney, P. D., Sivashinsky, G. I., A Theoretical Study of Propagation and Extinction of Nonsteady Spherical Flame Fronts, *SIAM Journal on Applied Mathematics, 49*.(1989), 4, pp. 1029-1046
[20] Bradley, D., *et al*., Burning Velocities, Markstein Lengths, and Flame Quenching for Spherical Methane-Air Flames: A Computational Study, *Combustion and flame, 104* (1996), 1-2, pp. 176-198
[21] Clavin, P., Dynamic Behavior of Premixed Flame Fronts in Laminar and Turbulent Flows, *Progress in energy and combustion science, 11* (1985), 1, pp. 1-59
[22] Hu, X., *et al*., Investigation of Laminar Flame Speeds of $CH_4/O_2/CO_2$ Mixtures at Ordinary Pressure and Kinetic Simulation, *Energy, 70* (2014), June, pp. 626-634
[23] Wang, H., *et al*., High-Temperature Combustion Reaction Model of H_2, in: *High-Temperature Combustion Reaction Model of H_2*. CO/C1-C4 Compounds, 2007
[24] Chu, H., *et al*., Effects of N_2 Dilution on Laminar Burning Velocity, Combustion Characteristics and NO_x Emissions of Rich CH_4–Air Premixed Flames, *Fuel, 284* (2021), 119017
[25] Xie, M., *et al*., Numerical Analysis on the Effects of CO_2 Dilution on the Laminar Burning Velocity of Premixed Methane/Air Flame with Elevated Initial Temperature and Pressure, *Fuel, 264* (2020), 116858
[26] Chen, J., *et al*., Kinetic Analysis of Laminar Combustion Characteristics of a H_2/Cl_2 Mixture at CO_2/N_2 Dilution, *ACS Omega, 7* (2022), 8, pp. 7350-7360
[27] Li, Q., *et al*., Measurements of Laminar Flame Speeds and Flame Instability Analysis of 2-Methyl-1-Butanol–Air Mixtures, *Fuel, 112* (2013), Oct., pp. 263-271
[28] Liu, Q., *et al*., Parameter Extraction from Spherically Expanding Flames Propagated in Hydrogen/Air Mixtures, *International Journal of Hydrogen Energy, 44* (2019), 2, pp. 1227-1238
[29] Smith, G.P., *et al*., GRI 3.0 Mechanism, Gas Research Institute (http://www. me. berkeley. edu/gri_mech), 1999
[30] Smith, G. P., *et al*., Foundational Fuel Chemistry Model Version 1.0 (FFCM-1), epub, accessed July, 26. (2016), p. 2018
[31] Li, X., *et al*., Uncertainty Analysis of the Kinetic Model Prediction for High-Pressure H_2/CO Combustion, *Proceedings of the Combustion Institute, 35* (2015), 1, pp. 617-624
[32] Rose, H., The Effects of Affirmative Action Programs: Evidence from the University of California at San Diego, *Educational Evaluation and Policy Analysis, 27* (2005), 3, pp. 263-289

Paper submitted: April 18, 2022
Paper revised: June 15, 2022
Paper accepted: June 20, 2022